

# CFD Simulation Of Hydrodynamics And Heat Transfer In Flow Of Liquids On Inclined Plates

Veeranna Modi <sup>1\*</sup>, Omprakash Hebbal <sup>2</sup>

<sup>1\*</sup>PG Student, Thermal Power Engineering, PDA College of Engineering, Gulbarga-585102, Karnataka (INDIA)

<sup>2</sup>Professor, Department of Mechanical Engineering, PDA College of Engineering, Gulbarga-585102, Karnataka (INDIA)

## ABSTRACT

A two phase flow CFD model using VOF method is used to predict the hydrodynamics and heat transfer of the continuously flowing liquids on inclined plates, corresponding to the surface of texture of structured packing. The behaviour of the flowing liquids under the influence of the plate microstructure, liquid properties and counter current gas is investigated. Heat transfer analysis is also carried out. From the simulated results it was found that, the liquid flow behaviour is dependent on the plate microstructure in absence of the counter current gas flow. Optimum speed of the counter current gas flow results in beneficial increase of the liquid flow thickness. High counter current gas flow speeds are undesirable, as the liquid flow thickness reduces and the flow pattern is badly affected. Addition of optimum height of wavy structure has enhanced the heat transfer between the surface and the fluids.

**Key words:** CFD; two phase flow; plate microstructure; heat transfer.

### Abbreviations-used:

ELO: Extra light oil; LDO: Light Diesel Oil;  $Re_L$ :Liquid Reynold's number; G:Gas flow velocity

## 1. Introduction

Liquid flow play an important role in many industrial applications. The thickness and velocity of liquid flowing down on vertical or inclined surfaces are among the key parameters determining overall performance of gas-liquid contacting apparatuses such as film evaporators, distillation columns, nuclear reactors, boilers, condensers, carbon capture & storage devices etc. The efficiency, rates of momentum and heat transfer of the packed columns is strongly influenced by the flow behavior of liquid film, fluid physical properties, presence of surfactants inside the packing. Many researchers have used the CFD to study the same and have verified the results with that of costly experimental. The result was satisfactory. With the recent computational developments, CFD is used to investigate the flow behaviour and the heat transfer characteristics. Some experimental and theoretical research work has been carried out in recent years, with the use of the

working fluids such as water, glycerol, acetone, ethanol etc. with and without counter current air flow. In this present work a study is carried out with the use of the oils like, LDO, ELO and also water on an inclined corrugated plate. The influence of solid surface microstructure, liquid properties, gas flow rate on flow behavior and the heat transfer characteristics are investigated

M.R. Khosravi Nikou *et.al.*[1], carried out a two phase CFD simulation using the Water-Air mixture, Glycerol-Air mixture and Methanol-Isopropanol, and studied the film flow behavior. It was found that by increasing liquid Reynolds number, the local maximum value of Nusselt number increase.

F Fang Gu et al [2] They carried out the CFD simulation on different liquids like water, glycerol, acetone, and ethanol are used to cover a range of liquid properties. It is found that increase in the liquid viscosity increase the liquid film thickness.

Then they have studied the influence of the counter current air flow and found that the free surface of the liquid film (acetone) initially begins to fluctuate but remains continuous. Then gradually as the time elapses, the liquid film breaks and drops appear when the acetone solution is used. Then the dry patches appear. Thicker film remains continuous even at the high gas flow rates.

J.J.Cooke et.al [3] studied the flow simulation on the inclined plate with monoethanolamine solution and found Surface texture significantly increases the wetted area of the plate. At lower Reynolds number, addition of the ridges to the plate causes channelling of flow which reduces the surface area minimising the effect of the surface tension

Yuanyuan xu et.al [4] used fluids on inclined plate such as toluene ,water, air and studied the Influence of the Liquid flow rate and found that, with a higher Reynolds number water forms a closed stable film. With the decrease in the Reynolds number water film breaks up and a rivulet flow appears.

The objective of the present work is to use the oils such as ELO, LDO in the liquid flow simulation. The water is used to cover range of liquid properties in case of influence of the plate microstructure on flow behavior. Water is also used in the heat transfer simulation.

## 2. Methodology.

As the VOF method is used in the present study, it is explained briefly. In computational fluid dynamics, the volume of fluid method (or in short VOF method) is a numerical technique for tracking and locating the free

surface (or fluid-fluid interface). It belongs to the class of Eulerian methods which are characterized by a mesh that is either stationary or is moving in a certain prescribed manner to accommodate the evolving shape of the interface. As such, VOF is an advection scheme a numerical recipe that allows the programmer to track the shape and position of the interface, but it is not a standalone flow solving algorithm. The Navier Stokes equations describing the motion of the flow have to be solved separately.

### 2.1 Governing equations

The mass, momentum and energy conservation equations for two-phase flow throughout the domain are:

$$\frac{\partial}{\partial t}(\rho) + \nabla \cdot (\rho \vec{v}) = 0$$

$$\frac{\partial}{\partial t}(\rho \vec{v}) + \nabla \cdot (\rho \vec{v} \vec{v}) = -\nabla P + \nabla \cdot [\mu(\nabla \vec{v} + \vec{v}^T)] + \rho \vec{g} + \vec{F}$$

$$\frac{\partial}{\partial t}(\rho h) + \nabla \cdot (\rho \vec{v} h) = \nabla \cdot (k \nabla T) + \frac{Dp}{Dt} - [\mu(\nabla \vec{v} + \nabla \vec{v}^T) : \nabla \vec{v}] - \nabla \cdot \left( \sum_k h_{k,j_k} \right)$$

The equations given above are dependent on the volume fraction of all phases, expressed implicitly by the properties  $\rho$  and  $\mu$ . In a two-phase system, for example, if the phases are represented by the subscripts 1 and 2 and the volume fraction of phase 2 is known, the density and viscosity in each cell are given by equations .

$$\rho = \alpha_2 \rho_2 + (1 - \alpha_2) \rho_1$$

$$\mu = \alpha_2 \mu_2 + (1 - \alpha_2) \mu_1$$

In the VOF model the movement of the phase interface is affected by the distribution of aq, the volume fraction of q<sup>th</sup> phase (secondary phase) in a computational cell. When in a particular computational cell aq=0 the cell is empty of q<sup>th</sup> fluid, and when aq=1 the cell is full of q<sup>th</sup> fluid. When 0 < aq < 1 the cell

contains the interface between the  $q^{\text{th}}$  fluid and one or more other fluids (Hirt and Nichols (1981). Thus, the interface between two phases can be traced by solving the continuity equation for the volume fraction function:

$$\frac{\partial a_q}{\partial t} + \vec{v} \cdot \nabla a_q = 0$$

The volume fraction for primary-phase in Eq. (6) will be obtained from the following equation:

$$\sum_{q=1}^n a_q = 1$$

## 2.2 Model geometry and Boundary conditions

To investigate the influence of the microstructure of the plate, a flat and the wavy plates listed in the table were used. Model geometry and the dimensions are given in the table 1 and the figure 1. No slip boundary condition is applied for all the plates at wall. The liquid is injected from a 3mm hole at the top and the gas is passed into domain from the bottom, flowing counter currently to the liquid. The constant fluid velocities are specified for the liquid and gas at inlet and the outlet. The free slip wall settings are used in the simulation. Liquid and the gas inlet temperatures are specified as atmospheric temperatures and the constant heat flux on the wall is specified in case of the heat transfer analysis. The symmetry boundary condition is used. The grids used in the simulations are hexahedra. The inclination angle for all the plates is set  $45^\circ$ .

## 2.3 Simulation Scheme

The CFD software Ansys CFX 13.0 was used in the simulation of continuous flowing liquids on various plates. The flow is transient flow, so the time dependent computations are carried out by

the software. About  $10^4$  to  $10^5$  time steps are necessary for the convergence. Second order upwind differencing scheme was chosen as the solution of the momentum equations.

The gas velocity is set to zero except in the case of the counter current gas flow simulations. The liquids are passed from the top. The gas is passed from the bottom in case of the counter current gas flow. The simulation process is carried out in unsteady conditions. The behavior of the different liquids under different influences such as the plate microstructure, counter current gas and liquid property at constant liquid Reynold's number can be observed.

**Table 1:** Structural parameters of plates. (7)

Configuration	Structural parameter		
	a [m]	a [m]	a/λ
Flat plate			
Wavy plate 1	0.00025	0.004	0.0625
Wavy plate 2	0.0005	0.008	0.0625
Wavy plate 3	0.0005	0.004	0.125
Wavy plate 4	0.001	0.008	0.125

**Table 2:** Physical properties of liquids.

Liquid	$\rho(\text{Kg/m}^3)$	$\mu(\text{kg/ms})$	K(w/mk)	$C_p(\text{KJ/Kg-k})$
ELO	809.1	0.005663	0.1453	1.967
LDO	892.31	0.0089	0.1323	1.779
Water	998.2	0.001003	0.6069	4.181

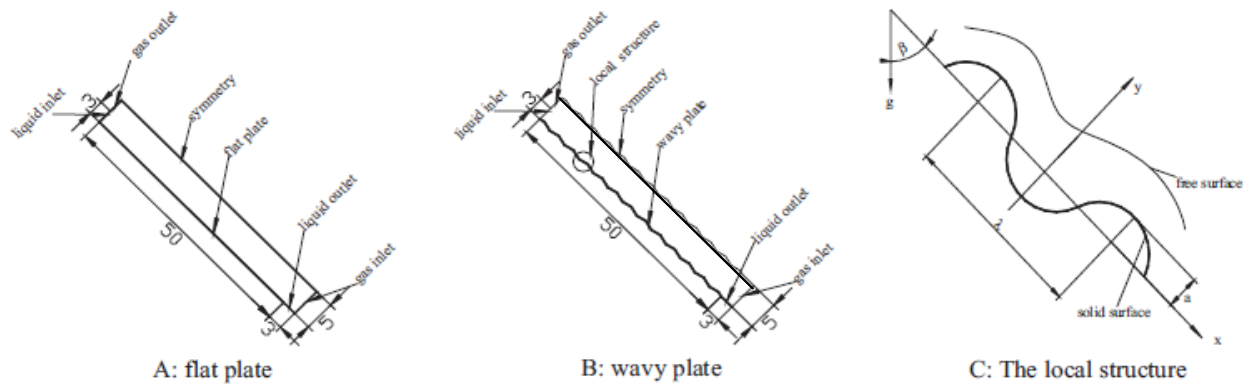


**Figure 1:** Model geometry and boundary conditions.

**3. Results and Discussions.**

**3.1: Effect of plate structure**

The CFD simulations are performed for the flow of water, extra light oil and light diesel oil on the five plates of different microstructure. The structural parameters have been listed in the table 1. The liquid properties are as listed in the table 2. All the three liquids are passed at the same Reynold’s number of 332 and the gas flow at 0 m/s in the simulation.

- Flow behavior for water.

The flow of water is smooth over the flat plate. At initial stage the accumulation of the water at the front of flow is less as compared to the flow at the end of the domain. The thickness of the water flow at front has increased at time instant of 0.45 s.

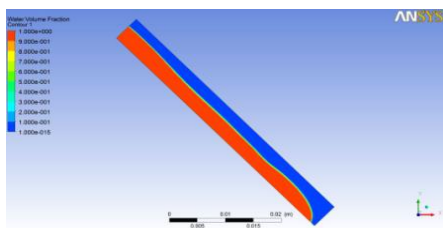


**Figure 2:** Water flow on flat plate (( $Re_L=332$ ;  $G=0$  m/s)

Wavy plate 1: As the water is flowing continuously, the flow is smooth. The streamlines are almost parallel to the microstructure of the plate. No eddies are formed in the concaves. The flow is in touch with the

bottom surface of the flow domain. Enlarged view of the flow near the concave is shown in the figure 4(a).

Wavy plate 2: Small eddies are formed in the concaves of the wavy structure. The flow is smooth over these eddies. Flow domain of the liquid is found slightly lifted above eddies. Enlarged view of the flow near the concave of the wavy structure is shown in figure 4 (b).

Wavy plate 3: In this case also eddies are formed in the concaves of the wavy structure but have more height in comparison to those in wavy plate 2. This says that the amount of liquid dead stock in concaves is more in comparison to that in wavy plate 2. The flow domain is above these eddies. This is illustrated in the figure 4(c).

Wavy plate 4: In this case the surface of the water almost acquires the nature of the wavy structure. As the plate has highest amplitude of all the plates, the water initially dumps and then rises up in the concaves. Eddies formed in the concaves are biggest compared to those formed in the wavy plates 2 and 3. Thus the water dead stock is also high in concaves, which is undesirable. The flow on this plate has been shown in figure 3 below.

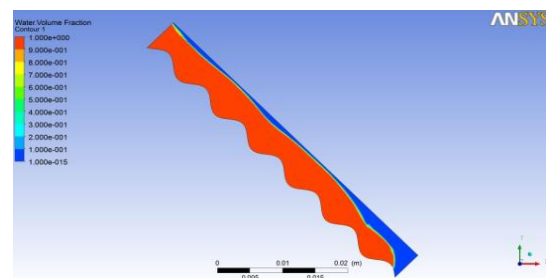
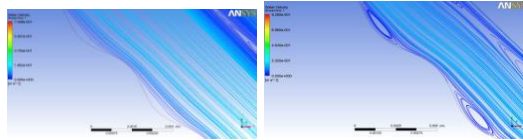
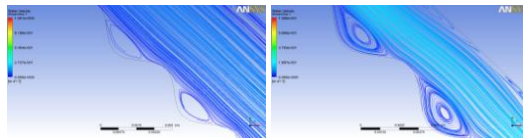


**Figure:3:** flow of water on wavy plate 4 (  $Re_L=332$ ;  $G=0$  m/s)

The streamline plots for all the 4 wavy plates are shown in figure below.



(a)Wavy plate 1 (b) Wavy plate 2



(C) Wavy plate 3 (d) Wavy plate 4

**Figure: 4:** Streamline plots for wavy plates.

From the above discussion of the results it is found that, adding too much wavy structure is undesirable as it increases the amount of stagnant liquid in the concaves.

#### Flow behavior of extra light oil (ELO)

In this case ELO of the properties listed in the table number 2 has been passed in the liquid flow domain of all five different plates listed in the table 1, at Reynold's number 332 and the gas flow at 0 m/s. Then the behavior of the flow is studied.

**Flat plate:** The flow of ELO is smooth. The oil starts to accumulate in the front end of the flow. Free surface of the oil is also smooth. As the oil travels further the air is trapped between the bottom layer of the oil and the bottom surface of the plate. Thus this forms small air bubble in the flow, which shall be carried forward by the flow.

**Wavy plate 1:** At initial stage of the oil flow, the oil accumulates at the front end. The bottom layer of the oil just touches the peak points of the wave structure. Thus the air which was present in the concave of the wave forms air bubble. But the oil at back of the air bubble touches the wave surface. Thus formed bubbles are carried forward in the flow. This phenomenon occurs at initial stage of the flow. Once all the bubbles are carried forward, the flow is smooth and the

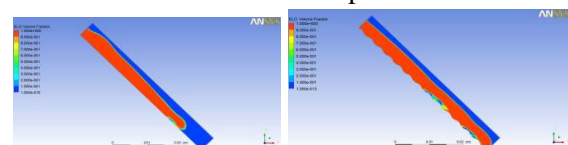
streamlines are parallel to the wave surface. No eddies are formed in the concaves of wave surface.

**Wavy plate 2:** The initial stage of flow is almost similar to that in the wavy plate 1. But the bottom surface oil flow dumps in the concaves at one wavelength distance. At this point small eddies are observed. The dumped oil rises up in tangent to the wave surface and reaches the next wavelength distance. Thus eddies are formed at alternative wavelength of the wave surface. The air bubbles formed are carried forward by the oil.

**Wavy plate 3:** At initial stage of the oil flow, the oil passes over the peak points of the wave surface. Thus the phenomenon of the air bubble formation happens here also. But the bottom layer of the oil is sheared by the peak points of the wave surface. Oil accumulates in the front of the flow. The accumulated oil due to its self weight dumps in the concaves. This is observed at every 2 wavelengths of the wave surface.

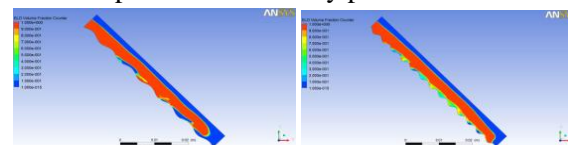
**Wavy plate 4:** The oil enters the domain in tangential to the wavy surface. It rises up to the top surface of the flow domain and continues to flow in the same position till the end of the domain. It falls down at the liquid outlet. This forms the large sized air bubbles than those in the wavy plates 2 and 3.

The following figure shows the simulated results for the ELO over all the five plates.



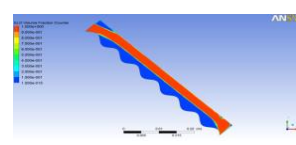
Inclined plate

Wavy plate 1



Wavy plate 2

Wavy plate 3



Wavy plate 4



**Figure 5:** The flow behavior of ELO over different plates ( $Re_L = 332$ ;  $G=0$  m/s)

### ➤ Effect of liquid properties

CFD simulations are carried out for liquids water, ELO and LDO to cover different viscosities and the densities listed in the table number 2. For all the three liquids the Reynold's number is kept constant ( $Re = 332$ ). The gas flow is maintained at 0 m/s.

We have

$$Re = u L / \nu = \rho u L / \mu$$

Where,

$Re$  = Reynolds Number (non-dimensional)

$\rho$  = density ( $kg/m^3$ )

$u$  = velocity based on the actual cross section area of the duct or pipe (m/s)

$\mu$  = dynamic viscosity ( $Ns/m^2$ )

$L$  = characteristic length (m)

$\nu$  = kinematic viscosity ( $m^2/s$ )

This gives  $u = (Re \nu) / L$

So  $u \propto \nu$ , therefore, as the kinematic viscosity increases, the flow velocity of the liquids increases when the  $Re$  number is kept constant. Then the liquid which has high kinematic viscosity flows faster than that liquid having less viscosity. According to the above concept, the simulations are carried out for the Water, ELO and LDO are performed. Among these three liquids the LDO flows faster than the other two. This is shown below in the figure 6.

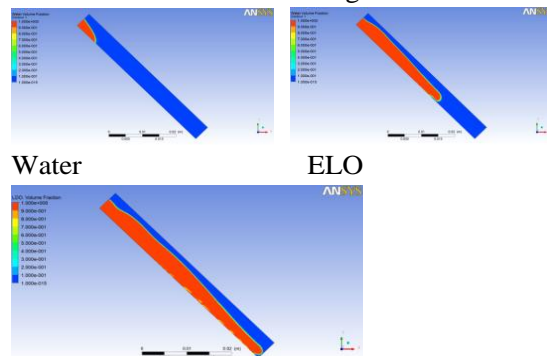


**Figure 6:** Simulation snap shots at 0.05 s for Water, ELO and LDO.

By the observation of the above snapshots, it reveals that the LDO has reached the liquid outlet, ELO is approximately at 65 to 70 % of the travel length and the water has begun to travel at 0.05 s.

### ➤ Effect of counter current gas flow on liquid flow behavior.

The effect of counter current gas flow on the ELO flow behaviour on wavy plate number 1 listed in the table 4.1 is simulated using Ansys CFX 13.0 software. Simulations are carried out for the liquid Reynold's number 332 and various counter current gas flow rates at 1 m/s, 1.2 m/s, 1.4 m/s, 1.5 m/s and 2.0 m/s.

At  $G=1$  m/s: The ELO at Reynold's number 332 and the counter current gas flow of 1 m/s are made to flow in the CFD simulation. The oil flow is smooth throughout its travel towards the liquid outlet. Slight increment in the thickness of the flow is observed at the end i.e. near the liquid outlet. The volume fraction contour of ELO is shown in the following figure 7.

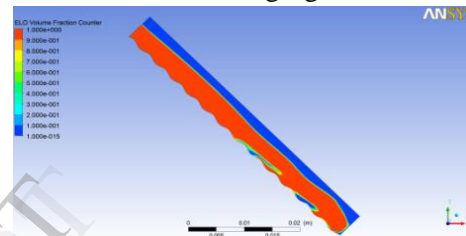


**Figure 7:** Volume Fraction contour for ELO ( $Re_L = 332$ ;  $G=1$  m/s)

At  $G= 1.2$  m/s: In this case the gas flow of 1.2 m/s and ELO at  $Re. = 332$  are set in the simulation. The nature of the flow is almost similar to that with gas flow of 1 m/s. But the flow thickness near the liquid outlet is slightly higher than that with gas flow of 1 m/s. But the thickness has not reached the top surface of the flow domain. This is illustrated in the following figure 8.

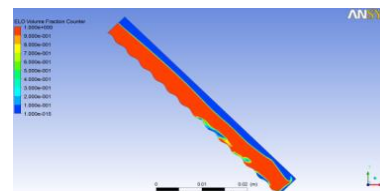
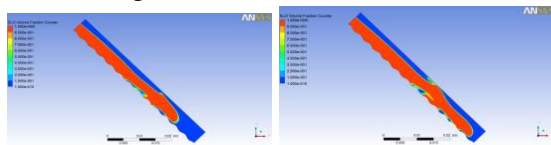


**Figure 8:** Volume Fraction Contour for ELO at ( $Re_L = 332$ ;  $G=1.2$  m/s).

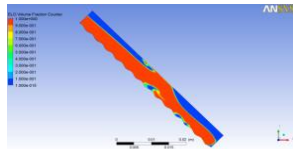
The counter current gas flow is increased to 1.4 m/s and the ELO is made to flow with same liquid Reynold's number of 332 in the simulation. The changes in the flow behavior

were observed. The surface of the flow at 0.062 s, starts to fluctuate and the top surface of the oil is pushed by the counter current gas. Thus the thickness of the flow increases and reaches the top surface of the flow domain. As the oil blocks the flow path of the gas due to increment in its flow thickness, the oil is pushed back. Then this oil rises back. Thus the flow path of the gas is blocked. But the oil makes the path to flow and reaches the liquid outlet end. The stages of the flow of oil at gas flow of 1.4 m/s are shown below in figure 9.



Snap at 0.06s

Snap at 0.073 s



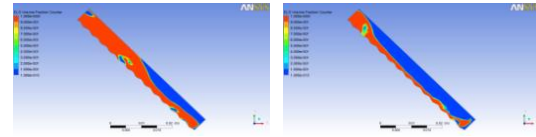
Snap at 0.077 s

**Figure 9:** Volume fraction Contours for ELO at ( $Re_L = 332$ ;  $G = 1.4$  m/s).

At  $G = 1.5$  m/s : The simulation is carried out for ELO at Reynold's number 332 and the counter current gas flow of 1.5 m/s. The flow behaviour is almost similar to that explained at gas flow of 1.4 m/s. But the surface fluctuation and the thickening of oil flow begins early i.e. at 0.055s. This phenomenon was observed at 0.062s for gas flow of 1.4 m/s. But another change observed is the thickness of the oil flow after the phenomena is less than that was observed in case of gas flow of 1.4 m/s.

At  $G = 2$  m/s : The simulation is carried out for ELO at Reynold's number 332 and the counter current gas flow of 2.0 m/s. The flow behaviour is almost similar to that explained at gas flow of 1.5 m/s. but the surface fluctuation and the thickening of oil flow begins early i.e. at 0.041s. This phenomenon was observed at 0.055s for gas flow of 1.5 m/s. But another change observed is the thickness of the oil flow after the phenomena is less than that was observed in case of gas flow

of 1.5 m/s. This is undesirable from the heat transfer and the mass transfer point of view. This is shown in the following figure 10.



( $Re_L = 332$ ;  $G = 1.5$  m/s) ( $Re_L = 332$ ;  $G = 2.0$  m/s)

**Figure 10:** Volume Fraction Contours for ELO. Hence optimum speed for the counter current gas flow must be adopted depending upon the process requirements.

- LDO flow behavior at counter current gas flow of 1.4 m/s.

One more simulation for the effect of counter current gas flow behavior is carried out for LDO at liquid Reynold's number 332 and counter current gas flow at 1.4 m/s. But the oil flow is not fluctuated at any instant of time throughout its flow. It is not pushed back and no reduction in the thickness of the oil flow is observed. This is due to the increase in the viscosity of the oil. The following figure 11 shows the behavior of the flow.

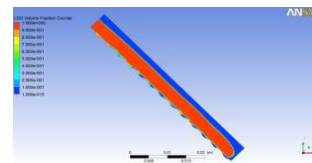


**Figure 11:** Volume Fraction for LDO ( $Re_L = 332$ ;  $G = 1.4$  m/s)

Thus it can be concluded that as the viscosity increases the film thickness increases and the force required to push the oil back is more.

- **Heat transfer characteristics**

Two phase flow CFD simulations are performed using the water on flat and wavy plate number 2 with various liquid Reynold's numbers of 332, 600, 900, 1200 and 1500. A constant heat flux of 600 w/m<sup>2</sup> boundary condition is applied on the wall. The water is passed into the domain at 298 k for all liquid Reynold's numbers. The gas flow is 0 m/s maintained at 298 k temperature.

The Nusselt numbers are calculated using the following procedure.

From Newton's law of cooling,

$$Q = h A (T_w - T_b)$$

Where

Q—Rate of heat transfer from the plate surface to the liquid--- (W)

h---Heat transfer coefficient--- (W/m<sup>2</sup> K)

A---Surface area of heat transfer---(m<sup>2</sup>)

T<sub>w</sub>—Average wall temperature---- (K)

T<sub>b</sub>---Average liquid temperature--- (K)

The above formula can be written as,

$$h = q / (T_w - T_b)$$

Where

q—heat flux on the surface of the plate--(W/m<sup>2</sup>)

$$T_b = (T_i + T_o) / 2$$

Where, T<sub>i</sub> ---liquid inlet temperature (K)

T<sub>o</sub>---liquid outlet temperature (K).

The T<sub>o</sub>, q and T<sub>w</sub> values are obtained from the CFD simulation. These values are used in the calculation of 'h'.

Then the Nusselt number is calculated for each case using the formula,

$$Nu = hL / k.$$

Where L= characteristic length = 0.03m.

K= thermal conductivity (W/m-K).

After the follow of the above said procedure the results are plotted with a graph of Nusselt number versus Liquid Reynold's number for flat and wavy plate number 2, where water was used in the simulation.

The graph is shown in the figure 12.

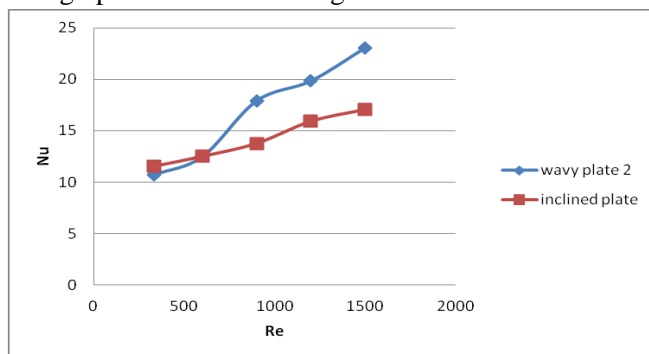


**Figure 12:** Nusselt number versus Liquid Reynold's number for flat and wavy plate number 2.

From the calculations and the graph results, it can be concluded that

- Increase in the Reynold's number has increased the Nusselt number.

- The rate of heat transfer has increased as the liquid Reynold's number has increased.
- The rate of heat transfer is increased after the addition of the waviness to the plate.

#### 4. Conclusions

- Addition of too much wavy structure is undesirable as it increases the amount of stagnant liquid in the concaves.
- In case of oils, as the viscosity and other properties varies, the oil flow behavior is different from that of water. The results are discussed above.
- The liquids with high viscosity flow faster than that with low viscosity, when the liquid Reynold's number is kept constant.
- Liquid flow thickness increases with the viscosity of the liquids.
- Optimum speed of the counter current gas flow is desirable as it just increases the flow thickness. But high speed of gas is undesirable which reduces the flow thickness affecting the process.
- High counter current gas flow is required for high viscous fluids.
- Increase in the Reynold's number has increased the Nusselt number.
- The rate of heat transfer is increased after the addition of the waviness to the plate.



## 5. References

- [1].M.R. Khosravi Nikou; 2008 ;5th European Thermal-Sciences Conference, Netherlands.
- [2].Fang gu, Chun Jiang Liu; 2004; Journal of Chem.Engg.Technology
- [3].J.J. Cooke, S. Gu, L.M. Armstrong; 2012; World Academy of Science, Engineering and Technology.
- [4].Yuanyuan Xu,Jingqi Yuan; 2012; J. Engg.applications of Computational Fluid mechanics.
- [5].S.Šinkūnas, A.Kiela; 2010; Effect of liquid physical properties variability on film thickness; Mechanika.
- [6].Kumar Subramanian, Steve Paschke; 2009; AIDIC conference series; vol.9; 2009.
- [7].S.Haeri, S.H. Hashemabadi; 2008; International Conference on continuum Mechanics.
- [8].Uwe Thiele, Edgar Knobloch; Physica D 190 (2004); science direct paper.
- [9].Kumar Subramanian; GunterWozny; International Journal of Chemical Engineering Volume 2012, Article ID 838965.
- [10].Hirt, C.W. and Nichols B.D., 1981, J. Comput. Phys.39, 201.
- [11].Computational fluid dynamics, J.D.Anderson Jr.
- [12].Bakker, Computational Fluid Dynamics Lectures; Multiphase flow, 2008).